Jpn. J. Appl. Phys. Vol. 41 (2002) pp. 336–345
Part 1, No. 1, January 2002

Positive DC Corona Discharge in N_2–NO–CO_2–O_2 Mixtures

Karol HENSEL, Nobuya HAYASHI, Chobei YAMABE and Marcela MORVOVÁ[1]

Department of Electrical and Electronic Engineering, Faculty of Science and Engineering, Saga University, 1 Honjo-machi, Saga 840-8502, Japan
[1]*Institute of Physics, Faculty of Mathematics, Physics and Informatics, Comenius University, Mlynská Dolina, Bratislava 842 48, Slovakia*

(Received April 2, 2001; accepted for publication October 1, 2001)

Positive DC corona discharge in a hemicylindrical discharge reactor was applied to mixtures containing N_2, NO, O_2, CO_2 and H_2O, while an NO_x chemiluminescence analyzer and an IR spectrometer were used to evaluate the concentration changes and analyze the products of the process in the discharge chamber. The removal efficiency of 89% for NO and the energy cost of 350 eV/molecule were achieved. Special attention was paid to the influence of CO_2 on discharge, its character, performance and products of the process. In addition to the main components of the gas mixture (NO, NO_2, CO_2, CO etc.), other compounds and functional groups (*e.g.*, amides I–III, imides, NCO) have been identified among the products of the process. [DOI: 10.1143/JJAP.41.336]

KEYWORDS: corona discharge, nitrogen oxides, carbon dioxide, IR spectrometry

1. Introduction

The increasing concern about the environmental problems the world is facing has enhanced interest in developing new and more effective gas cleaning technologies in recent decades. The environment is polluted by chemicals emitted directly from identifiable sources and by those formed indirectly through photochemical reactions in the air. The nitrogen oxides (NO_x) produced primarily by coal-burning power plants and diesel engines are considered to be one of the most aggressive chemicals. They contribute to air pollution, acid rain, photochemical smog production and the steadily increasing concentration of greenhouse gases in the atmosphere. Consequently, they also cause many serious respiratory diseases such as bronchitis and pneumonia.

Several methods have been proven efficient in removing NO_x from flue gas (electron beam irradiation, silent discharge, corona discharge, surface discharge, partial discharges and ferroelectric pellet bed); among them, corona discharge, particularly pulsed corona discharge, represents a very attractive alternative, as has already been demonstrated in several laboratory and pilot-scale experiments in recent decades. In conjunction with the laboratory experiments and pilot-scale tests, computer simulations are also being done to elucidate the mechanisms of chemical reactions responsible for the removal of pollutant compounds. The chemical reactions in a discharge environment are very complicated and hundreds of reactions are possible. In corona discharge induced plasma chemical processes the main role in played by electrons, radicals and ions. In addition, surface, thermochemical, heterogeneous and conventional chemical reactions also take place. Various authors,[1–12] have reported on laboratory experiments with regard to the effects of high-voltage waveform (its amplitude, shape, polarity), input power, initial pollutant concentration, residence time, gas flow rate, gas temperature, moisture, chemical additives, and the presence of surface discharge. The discharge conditions, chemical reactions, final products, energy consumption and efficiency of the process can be significantly influenced by changing these parameters.

Among various chemical additives used in the NO_x removal process (*e.g.*, NH_3 or hydrocarbons), the influence of CO_2 has been studied only partially. No detailed description of the effect of CO_2 on NO_x treatment process has been published yet, and the chemical reactions and products of the process still remain almost unknown. An extensive individual investigation of the CO_2 decomposition process in corona discharge has been, however, carried out, with a particular focus on mixtures with air.[13,14] Particularly good results were obtained using pulsed corona discharge in the presence of granular ferroelectric matter.

In processing the mixtures containing NO_x and CO_2 by corona discharge, it is believed that the NCO radical plays an important role.[15–17] The radical is responsible for the removal of NO_x, but can also be incorporated in various heterogeneous metal organic compounds formed on the surface of electrodes. Such compounds are effectively formed in particular on chemically active materials (*e.g.*, copper or brass) having significant catalytic properties. Moreover, in mixtures containing N_2–CO_2–H_2O, the eventual formation of some essential amino acids on the surface of electrodes was proved.[17] Here again the responsible agent appears to be the NCO radical, whose reaction with the H_2O (the presence of H_2O is necessary for the process) in the mixture leads to the formation of the amide group $^+NH_2$–COO^-, which is the first step in the formation of the essential amino acids (*e.g.*, glycine). The question is, however, whether similar processes also occur in the mixtures of NO_x–CO_2–H_2O, by which NO_x and CO_2 would be simultaneously removed.

The aim of the present research was to perform measurements in mixtures containing N_2, NO, CO_2, O_2 and water, describe the discharge process and identify the products. Our intention was to perform measurements using a positive DC corona discharge in different modes, however a positive DC streamer corona discharge was used predominantly. Although the elementary processes and chemical reactions are complicated and many of the products remain unknown, several facts about the discharge process, the analysis of the products and interpretations of the spectra are presented.

2. Experimental Setup

The experimental setup is presented in Fig. 1. A hemicylindrical-type corona discharge reactor with a length of 20 cm was employed in the experiment. The active electrode consisted of a copper or tungsten wire with 0.1 mm diameter and a copper hemicylindrical electrode with 35 mm

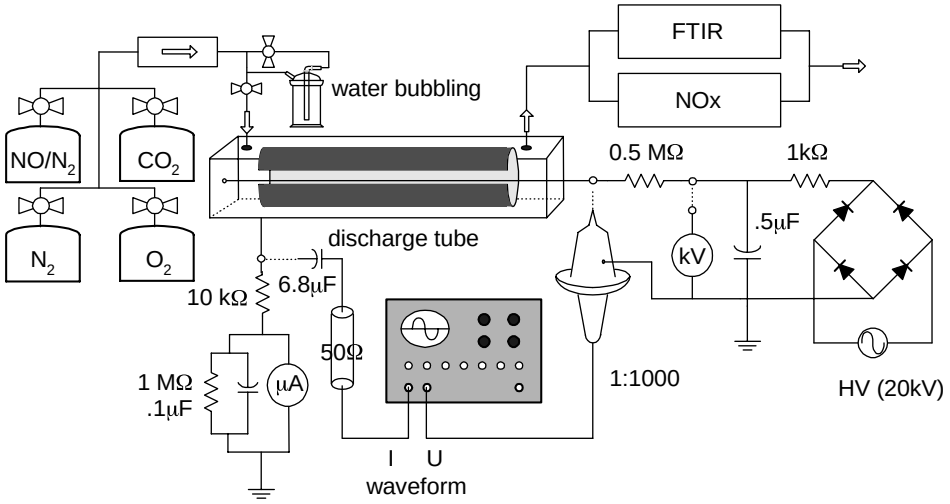

Fig. 1. Experimental setup.

diameter served as a passive (grounded) electrode. In order to avoid discharge breakdown at the sharp edges of the hemicylindrical electrode, extra copper elements with a large curvature of radius ('Rogowski designed') were mounted at both ends of the hemicylinder.

Conventional HV power supply was used together with a rectifying circuit and an RC integrator to produce a DC output signal. A DC streamer corona discharge mode of positive polarity was mainly used. The discharge voltage was monitored by a high-voltage passive probe (Tektronix P6015A) connected to an oscilloscope while the discharge current (both mean current I_m and current waveform) was recorded by an analog microampermeter and oscilloscope (Tektronix TDS380).

The composition of simulated gas was controlled by flow regulators on each of the high-pressure cylinders containing N_2, NO (500 ppm admixture in N_2 gas), CO_2 and O_2. For measurements with H_2O, a simple water bubbling system at room temperature was used, so the maximum concentration of the water vapor in the mixture was limited to approximately 3%. All measurements were performed in a flow regime with the total gas flow set to either 1 or 2 l/min. The concentrations of NO and NO_x in the gas mixture at the output of the reactor were continuously monitored by an NO_x chemiluminescence analyzer (Shimadzu NOA-7000) and the overall analysis of the products was done using an FT-IR spectrometer (Herschel/Jasco FT/IR-430). To improve the resolution of the measured IR absorption spectra, a 2.4-m-long gas cell (Gemini Mercury Cell #0.1L/2.4M) was used instead of a conventional 10 cm one.

3. Experimental Results

The overall experiment consisted of two parts. First, we performed several measurements in the gas mixtures containing N_2–NO–CO_2–H_2O, while deNO and deNO_x efficiencies were monitored by a NO_x chemiluminescence analyzer. This part of the experiment was performed to ascertain the general influence of CO_2, and also that of H_2O, on deNO_x efficiency and power consumption. Second, we concentrated on the overall analysis of all components of the gas mixture and analyzed the products formed in the discharge process with the use of IR spectrometry. For this purpose, we performed several measurements using different gas mixtures treated by a positive DC corona discharge (Table I).

Table I. Overview of mixtures treated by corona discharge and analyzed by IR spectrometry.

1	$\mathbf{N_2 + 20\%\ O_2 + x\%CO_2}$ ($x = 0, 1, 3, 5, 10, 20, 30, 50\%$)
2	$\mathbf{N_2 + 250\ ppm\ NO + x\%CO_2}$ ($x = 0, 1, 3, 5, 10, 20, 30\%$)
3	$\mathbf{N_2 + 250\ ppm\ NO + 20\%\ O_2 + x\%\ CO_2}$ ($x = 0, 1, 3, 5, 10, 20, 30\%$)

3.1 *Discharge character*

The effect of individual components of the gas mixture on the discharge character was very significant. Specifically, an admixture of 20% of O_2 in the gas mixture stabilized the discharge, transforming it from a streamer mode to a glow mode [Fig. 2(a)] as attachment processes became dominant. The oxygen in the initial mixture was also responsible for the decrease of discharge onset voltage V_o and the break-

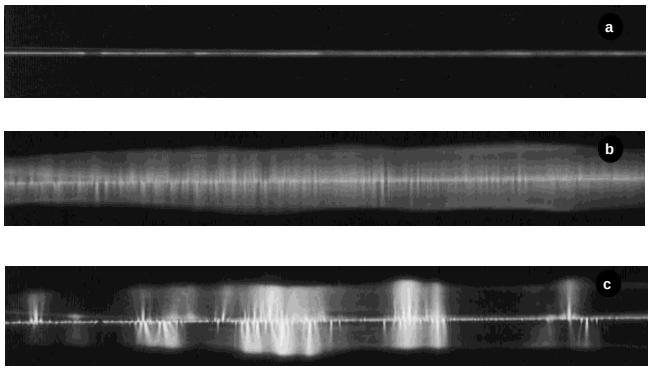

Fig. 2. Photographs of typical light conditions of discharge in different gas mixtures ($I_m = 1500\ \mu A$): (a) $N_2 + 20\%\ O_2$, (b) $N_2 + 250$ ppm NO + 20% O_2 + 20% CO_2, (c) $N_2 + 250$ ppm NO.

down hindering up to higher currents ($I_m > 1$ mA), compared with the discharge in pure nitrogen. The small increase of the mean current I_m in the N_2–O_2 mixture was evidently caused by O_2 molecule impact ionization. In contrast to the effect of O_2, the presence of only a low concentration of CO_2 in the initial mixture caused an increase of V_o and the streamer and the pulse behavior of the discharge gradually recovered with increasing concentration of CO_2 (the same effect was also observed in the mixtures with initial NO). The bright, homogenous light of the corona glow discharge along the wire disappeared little by little, while the number, intensity and repetition rate of emission spots and channels in the discharge gap progressively increased. The further increase of the concentration of CO_2 (up to 20%) caused the number of streamer channels to increase, thus filling the entire discharge gap between electrodes as shown in Fig. 2(b). While the amplitude and the duration of the streamer pulses decreased, the frequency of the pulses increased with increasing concentration of CO_2 (for the same value of the mean current I_m). The transition between glow and streamer can be very well controlled by CO_2 injection.

The admixture of NO, like O_2, caused a decrease of the corona onset voltage V_o and hindered breakdown (if compared to pure N_2). With increasing the discharge current, streamers gradually appeared with rapidly growing amplitude and frequency. Visually, the streamer channels in the discharge gap were brighter and more intense than those in N_2–O_2–CO_2 mixtures, though the density of emission spots and channels along the wire was lower [Fig. 2(c)]. An increase of CO_2 concentration in the initial mixture (up to 3–5%) caused the discharge utilization by streamers as well as their distribution in the discharge gap to become more homogenous.

There was a difference between the mixtures with and without NO in the initial mixture. In the mixtures with initial NO, streamers already occurred in the early stages of the discharge. The subsequent admixture of CO_2 enhanced the streamers, improving their space distribution in the discharge gap, while in the mixtures without initial NO (either pure N_2 or N_2–O_2), the streamers appeared only after CO_2 was introduced. Too much CO_2 caused the streamers to gradually die out in the gap, and the discharge light intensity faded and discharge instabilities occurred. With a very large amount of initial CO_2 injected, corona discharge onset voltage could be significantly increased and the streamer corona might terminate. Generally speaking, both O_2 and NO caused a decrease of onset voltage V_o, while the effect of CO_2 was the opposite. At the same time, the presence of NO and CO_2 supported the streamer mode, while injection of O_2 stabilized the discharge in the glow mode.

3.2 *Analysis of the gas mixtures*

The instant concentration of the nitrogen oxides in the gas mixture was measured by a chemiluminescence-type NO_x analyzer and also later by an FTIR spectrometer. The measurements using the NO_x chemiluminescence analyzer were performed to ascertain the general influence of CO_2 and partially that of H_2O on NO_x removal efficiency and power consumption. In the case of the N_2–NO (500 ppm) gas mixture and the total gas flow of 2 l/min, the maximal NO removal efficiency of 89% was obtained at the energy

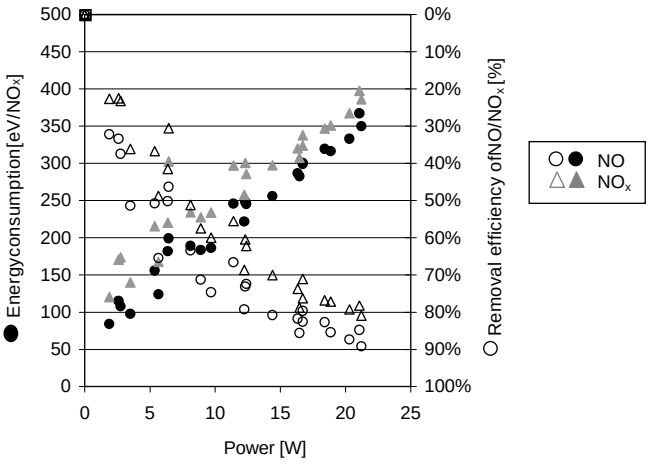

Fig. 3. Efficiency and energy consumption of deNO and deNO_x processes in N_2 + 500 ppm NO mixture.

consumption of 350 eV/NO (Fig. 3). At the same time, the overall deNO_x efficiency was approximately 81%, while the energy consumption of 386 eV/NO_x was achieved.

3.2.1 *Effect of CO_2 and H_2O on NO_x removal chemistry under the influence of the discharge*

The injection of CO_2 gas into the mixture led to a decrease of both NO and NO_x removal efficiencies and the increase of energy consumption per NO molecule removed in both dry and wet gas mixtures (Figs. 4 and 5). This was caused by a gradual change in the discharge character

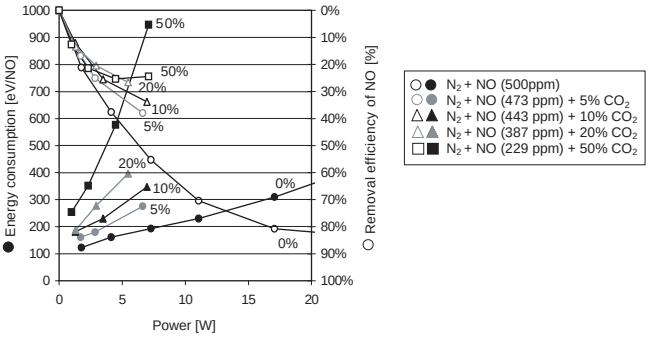

Fig. 4. Efficiency and energy consumption of deNO process in N_2–NO–CO_2 mixtures.

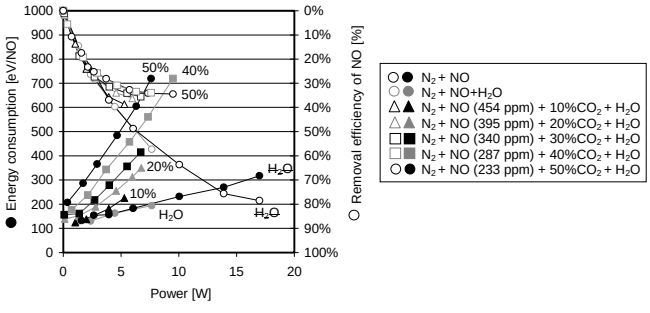

Fig. 5. Efficiency and energy consumption of deNO process in N_2–NO–CO_2–H_2O mixtures.

described earlier, and by the fact that CO_2 itself, along with other gas components, undergoes changes under the influence of the discharge action, while its concentration is several times higher than the concentration of NO_x. There is an essential difference between the process in the mixtures containing CO_2 and that in the mixtures without it.

In the *mixtures without CO_2*, the main reaction channel for NO removal is the production of NO_2 by $O(^3P)$ or O_3 and further oxidation to HNO_3 by OH radicals produced particularly by $O(^1D)$ from the water vapor. To some extent, the NO_2 can sometimes also be oxidized by O_3 or $O(^1D)$ [produced in the process of excitation of O_2 by electron impact and the subsequent dissociation into $O(^3P)$ and $O(^1D)$ state] to NO_3, while the subsequent reaction of NO_3 leads to the formation of the N_2O_5 ($NO_2^*NO_3$) complex. The complex, if formed, reacts with H_2O and forms $2HNO_3$. For both cases, the more HNO_3 is formed in the liquid phase, the more NO_2 can be formed in the gas phase and so the efficiency increases. This, in fact, is the influence of the water. The energy consumption of this process increases more or less linearly with the number of molecules oxidized.

In the *mixtures with CO_2*, however, this mechanism does not work for several reasons. Here, the primary oxygen is used for the oxidation of CO_2 and the formation of CO_3^- and CO_4^-, while the presence of water causes H_2CO_3 to be formed instead of CO_3.[13] In the case of the simultaneous presence of water and oxygen in the mixture, H_2O_2 is produced and its reaction with CO_2 leads to the formation of $(HCO)_4$ acid. This process also leads to a decrease in ozone production, as oxygen in the $O(^3P)$ state is necessary for H_2O_2 formation. Regarding the OH radicals, although only one oxygen atom is needed for their production, the oxygen must be in the $O(^1D)$ state that unfortunately requires more energy.

The presence of CO_2 causes the reactions responsible for the removal of NO to become much more complicated. First, there is an activation step involving the formation of an electronically excited metastable state of molecular nitrogen N_2 ($A^3\Sigma_u^+$) with an energy of 6.85 eV and a relatively long lifetime of 1.3–1.9 s.[18] This is achieved in two steps, which include repeated electron impact leading to the transition of molecular nitrogen from its ground state N_2 ($X^1\Sigma_g^+$) to the rotationally excited $C^3\Pi_u$ state with energy ~11 eV and subsequent de-excitation of this state by adiabatic transfer to the $A^3\Sigma_u^+$ metastable state.[19] In our type of discharge the production of $N_2^*(A^3\Sigma_u^+)$ is relatively significant,[20,21] although it is not the dominant process and it is also very sensitive to oxygen concentration and decreases with it.[22] In the discharge with the high pulse frequency, these metastable states are accumulated and serve as an energy reservoir for the subsequent chemical process. The activated N_2^* is incorporated into the CO_2 in the next step. For this process, the accumulated energy is necessary; however it is released after the stable molecule is formed (the process of energy recovery). The reaction of N_2^* with CO_2 leads to the formation of long-lived NCO, ON–NCO or similar intermediates. The ON–NCO can also be produced by the reaction of NCO with NO* respectively NO,[23,24] where $NO^*(A^2)$ is formed by energy transfer with the metastable $N_2(A^3\Sigma_u^+)$. If water is present in the system, the NCO reacts with it and trivial amino acids may be formed (Fig. 6). In the case where such an amino acid is formed, the energy is

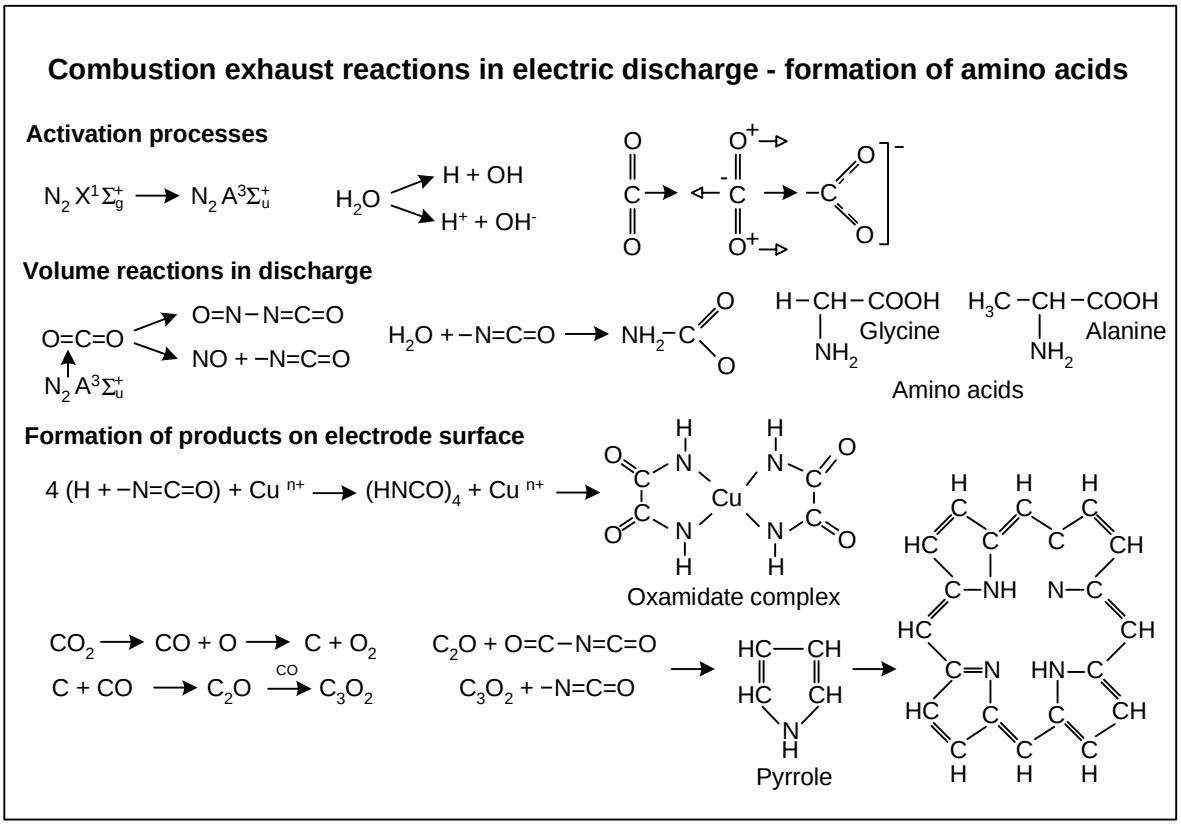

Fig. 6. Combustion exhaust reactions in the electric discharge-formation of amino acids.

released and can be used again, but only if the residence time of the gas mixture in the discharge system is sufficiently long. In the long-discharge reactors, the energy is recovered and the total energy consumption does not increase further, and it may decrease.[19)]

The *presence of H_2O* in the mixture of N_2–NO (without CO_2) improved the deNO$_x$ efficiency, as it enhanced the process of the direct oxidation of NO_2 to nitric acid and in addition also the process of nitric acid formation from N_2O_5. Although only a small change in the NO removal rate efficiency was observed, improvement of the NO_2 removal efficiency resulted in the improvement of the total NO_x removal rate. The effect of water is more apparent in the case of N_2–NO–CO_2 mixtures, where the injection of water caused an even greater relative improvement of both NO and NO_x removal efficiencies (Fig. 7). However, to describe the direct influence of water, in the case of the presence of CO_2 and without it, on the removal process of NO_x is far more complicated, because of the completely different mechanisms, development times and by-products of the processes. In the case without CO_2, the process goes through the production of N_2O_5 to the formation of acids in the reaction with water. In the presence of initial CO_2 and water, however, the initial phase is the production of NCO radical, and an ON–NCO intermediate, followed by the formation of amino acids and later the formation of polymers. While in the initial step the energy is consumed, during the production of polymers the energy is released. Because of the relatively short residence time, as it is unfortunately also in the presented system, some reactions remain incomplete. Therefore, to compare the energy consumptions or to talk about the influence of water in such a complex process and make a comparison with a simple process such as the formation of acid in the system without CO_2, is not useful. Moreover, as the complex process consists of many chain reactions under nonequilibrium conditions (since plasmochemical reactions are usually nonequilibrium reactions) to determine the reaction rate coefficients is in principle impossible and also for such processes the rate coefficients cannot be used.

Regarding the discharge character, no significant change was observed; only the slight decrease of the breakdown voltage in the presence of water (caused by its condensation on the surface of electrodes and its high ε_r) and the increased chance of discharge instability were observed. Generally,

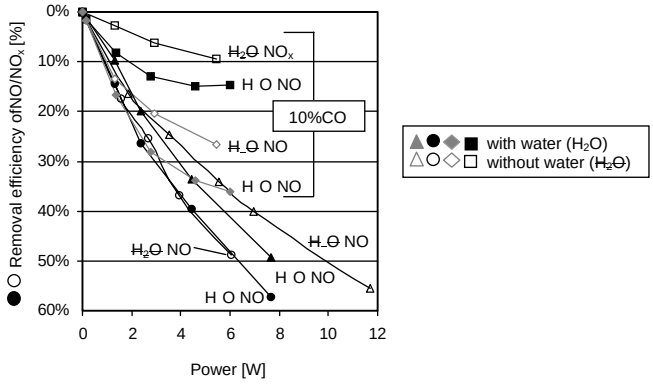

Fig. 7. Effect of water on the efficiency of deNO and deNO$_x$ processes in N_2–NO and N_2–NO–CO_2 mixtures.

Table II. Characteristic absorption bands of the main compounds of the gas mixture.

	IR absorption band (cm^{-1})
NO	**1905** monomer, 1845 dimer
NO_2	**1630**, 1605, 2930–2900 overtones
N_2O	**2235** (between CO_2 and CO bands)
CO_2	**2400–2300**, 3800–3700, 677
CO	**2170**, 2115

and in agreement with the chemical process described above, the presence of water vapor in the mixture as well as OH and HO_2 radicals produced by the dissociation of H_2O by high-energy electrons or generated by reactions of H_2O with O radicals, is believed to significantly promote the chemical process. The water vapor can also enhance the oxidation of nitrogen gas into N_2O[25)] and its presence is necessary for the formation of amino acids, as previously mentioned.

The analysis of the gas mixture by means of IR spectrometry is a very effective method for monitoring the changes of the gas mixture composition caused by electric discharge, and for product identification. The spectra of different kinds of initial gas mixtures treated by corona discharge (Table I) were recorded continuously with increasing discharge power. Although the molecules of O_2 and N_2 are infrared-inactive, the absorption bands of NO, NO_2, CO_2 and other chemical compounds and functional groups were detectable and clearly visible in the spectra. The absorption bands of the main components of the initial gas mixtures are presented in Table II. To improve the resolution of the spectrometric measurements of the gas mixture composition, a 2.4-m-long gas cell was used and the total gas flow rate was decreased to 1 l/min compared with the previous measurements (to increase the residence time). The concentration of NO in the gas mixture was reduced to half of the previous amount (250 ppm of NO), because a better reduction effect for NO and NO_x can usually be obtained with a lower initial NO concentration as radical reactions dominate the discharge (although a decrease of this concentration also results in an increase of energy consumption).

Figures 8(a) and 8(b) are the absorption spectra of two different mixtures treated by a positive corona discharge, where the overall effect of the discharge action on the gas composition can be seen. Each figure is composed of three spectra successively representing the pure N_2, the gas mixture before and the gas mixture after the discharge action (at $I_m = 1000\,\mu A$). The development of the individual concentrations of the main components in the gas mixtures with the increasing discharge power is presented in Figs. 9–12.

Based on the results of spectrometric measurements and the analysis of the spectra, the following conclusions can be made.

3.2.2 *Concentration of NO*

The removal process of NO (Fig. 9 presents the relative changes of the absorption band of NO at 1905 cm^{-1}) in the mixtures, without initial O_2 or CO_2, was strongly reductive with relatively low energy consumption. The dominant

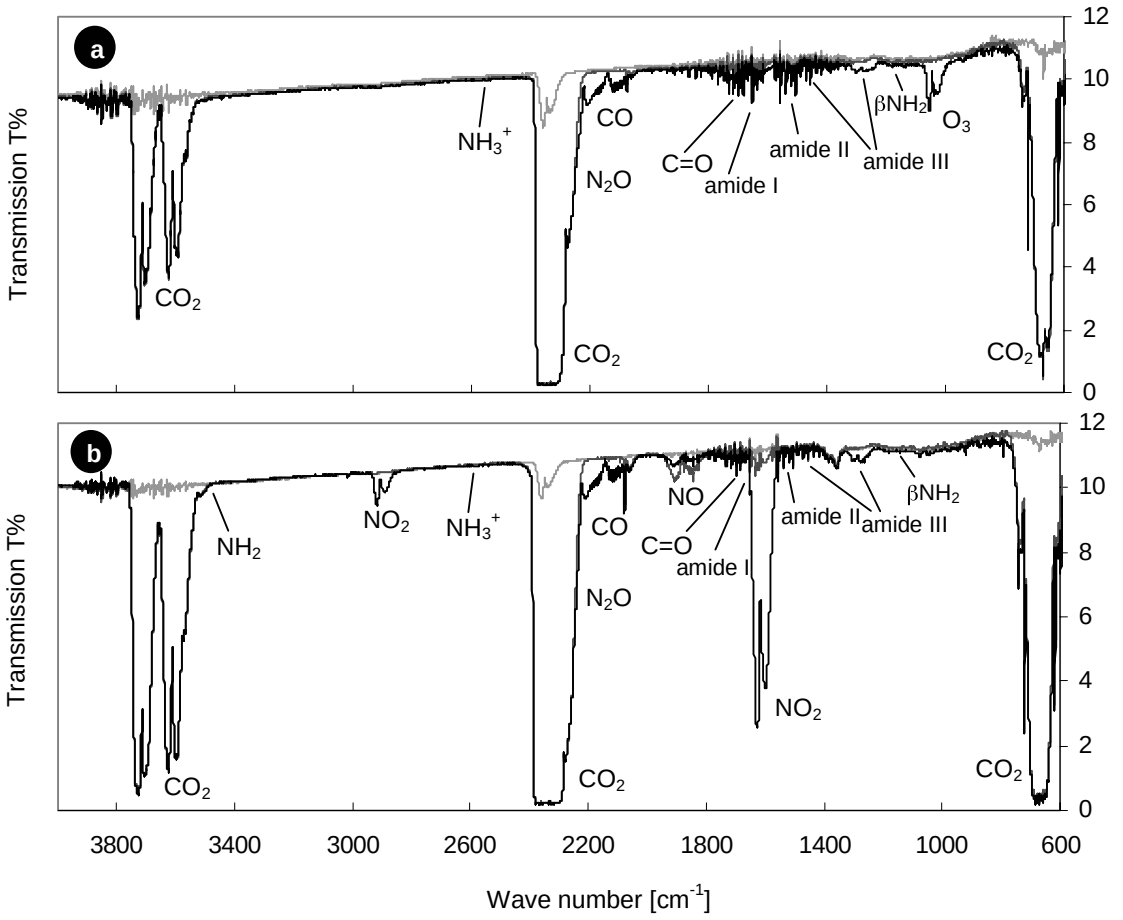

Fig. 8. Typical IR absorption spectra of mixtures containing CO_2 and NO treated by corona discharge: (a) $N_2 + 20\%\ O_2 + 1\%CO_2$, (b) $N_2 + 250$ ppm $NO + 20\%\ O_2 + 5\%\ CO_2$.

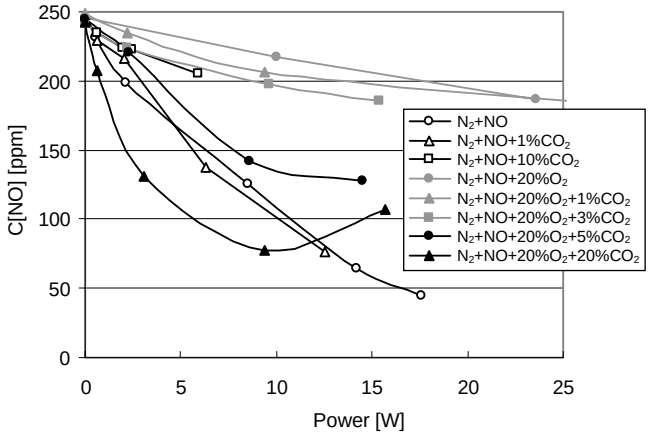

Fig. 9. Change of NO concentration caused by positive DC corona discharge in the gas mixtures containing N_2–NO–CO_2–O_2.

process here was the decomposition of NO into molecular oxygen and nitrogen, while a certain amount of N_2O (see below) was also produced. Likewise, a small amount of NO_2 was produced, which later decreased with increasing discharge power. A small amount of CO_2 (1%) in the initial mixture slightly improved the deNO efficiency, probably due to an increase of the streamer repetition rate, although at the same time the production of NO_2 increased. Further increase of the CO_2 concentration in the initial mixture had a negative effect on deNO efficiency, which was in agreement with the previous results obtained using the NO_x chemiluminescence analyzer. With 20% of O_2 in the mixture, the discharge first fell into the glow mode, resulting in a low NO removal rate, even with 1 or 3% CO_2 added. However, a further increase in CO_2 concentration helped to recover the streamer mode and to improve the deNO efficiency. This was also due to the enhanced oxidation of NO into NO_2.

3.2.3 Concentration of NO_2

The concentration of NO_2 (Fig. 10 presents the relative changes of the absorption band at $1630\,cm^{-1}$) apparently increased in all types of mixtures investigated, except for the later stages in the mixture with only N_2 and NO, where the NO_2 concentration decreased at very high discharge power. In the mixtures with initial NO and O_2, the concentration of NO_2 increased rapidly due to the immediate oxidation of NO to NO_2. Additionally, the influence of CO_2 is not negligible, as it is particularly evident in the measurements in N_2–NO–O_2–CO_2 mixtures. Its presence in the mixture improved the streamer mode discharge, which resulted in the enhancement of the chemical processes. In contrast, in the mixtures without initial NO, the streamer mode incepts only after CO_2 input and later vanishes with increasing CO_2 concentration. The concentration of CO_2 above 10% led to continuous streamer disappearance, contraction of the discharge to the

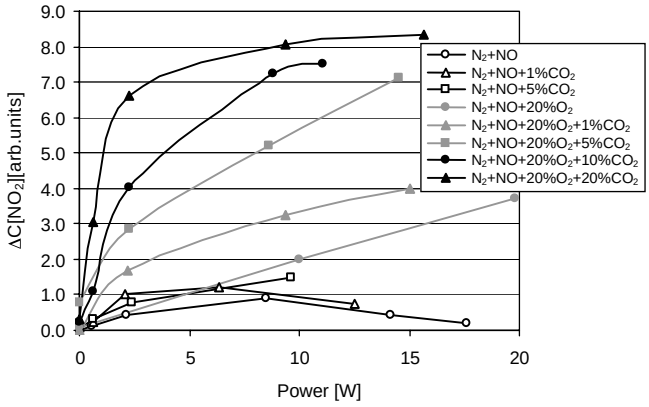

Fig. 10. Relative change of NO_2 concentration $\Delta C[NO_2]$ caused by positive DC corona discharge in the gas mixtures containing N_2–NO–CO_2–O_2.

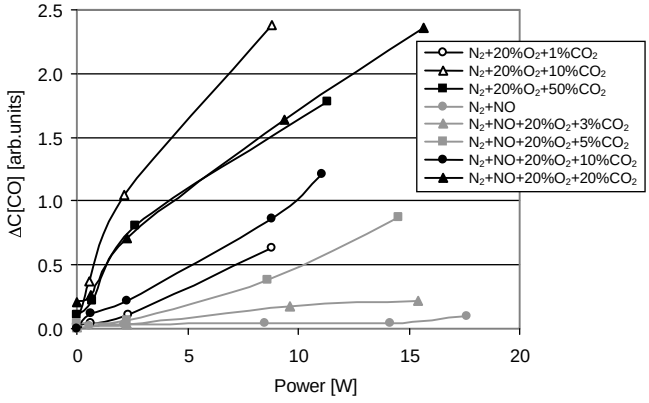

Fig. 12. Relative change of CO concentration $\Delta C[CO]$ caused by positive DC corona discharge in the gas mixtures containing N_2–NO–CO_2–O_2.

vicinity of the wire, and the formation of only a very small amount of NO_2.

3.2.4 *Concentration of N_2O*

The production of N_2O (Fig. 11 presents the relative changes in the absorption band at $2235\,cm^{-1}$) in the discharge process is also apparent. In the mixtures of N_2–NO–CO_2, although the discharge action caused relatively significant changes in the concentrations of both NO and NO_2, the concentration of N_2O hardly changed and remained low. However, the increase of N_2O production in the mixtures with the initial O_2 was caused mainly by the improvement of the discharge conditions and streamer corona discharge, rather than being due to any direct chemical reaction of oxygen with nitrogen oxides in such a way that N_2O would be produced. Thus, the most probable process for N_2O production remains the reaction $NO_2 + N \rightarrow N_2O + O$. An increase of CO_2 concentration in the mixture resulted in a decrease of N_2O present in the N_2–NO–CO_2 mixtures, probably caused by the continuous disappearance of the streamer discharge previously mentioned.

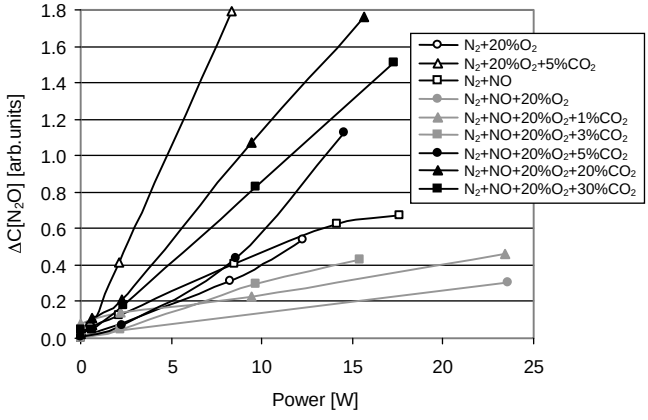

Fig. 11. Relative change of N_2O concentration $\Delta C[N_2O]$ caused by positive DC corona discharge in the gas mixtures containing N_2–NO–CO_2–O_2.

3.2.5 *Concentration of CO*

In the discharge process, CO was also produced (Fig. 12 presents the relative changes of the absorption band at $2170\,cm^{-1}$). Its concentration increased in proportion to the initial concentration of CO_2 in the mixture. The increase of CO concentration could also be caused by the decomposition of compounds and intermediates previously created in the discharge process (*e.g.*, ONNCO) due to the high frequency of the pulses.[26] The presence of water in the mixture, however, leads to a decrease of CO concentration. Likewise, in the case of N_2O, the presence of O_2 in the initial mixture together with CO_2 resulted in an intense streamer corona discharge, which indirectly affected the production of CO.

3.2.6 *Concentration of O_3*

In the case of N_2–O_2–CO_2 mixtures, an ozone doublet appeared in the region of 1050–$1030\,cm^{-1}$ [Fig. 14(a)]. Its concentration continuously increased with the CO_2 concentration as the result of CO_2 conversion into CO. In contrast, in the mixtures with initial NO, the ozone concentration was comparably lower. This was due to the fact that NO was oxidized to NO_2 both by $O(^3P)$ necessary for ozone production, and by ozone itself,[27] resulting in a limited concentration of ozone in the mixture. The generation of ozone can be strongly suppressed by a high concentration of water vapor (6% or more) and a high pulse frequency, similar to the case of CO production.

3.2.7 *Overall analysis of gas mixture*

In addition to the absorption bands of the major components of the gas mixture, other bands also appeared in the spectra. Through a complex analysis of the spectra, considering all possibilities, discharge conditions, and initial gas compositions as well as the intensity of absorption bands, other interesting compounds and functional groups were also identified. Although many reaction products with low extinction coefficients could not manifest themselves sufficiently in the absorption spectra of the mixture, the resulting analysis was satisfactory.

While analyzing the spectra and identifying the compounds, the possible formation of amino acids or at least some of their fractions and functional groups was also taken into account, as their formation in the discharge process had

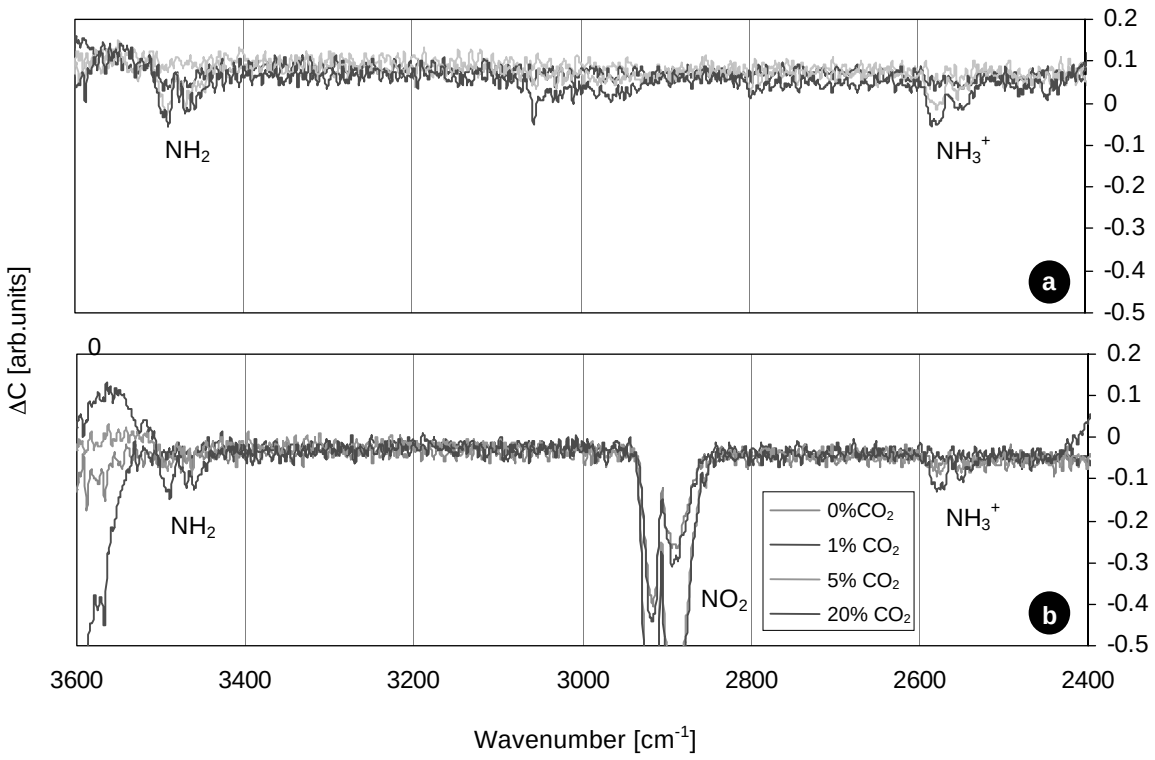

Fig. 13. Details of differential spectra of mixtures treated by DC positive corona discharge: (a) N_2–O_2–CO_2, (b) N_2–NO–O_2–CO_2. Each curve represents a different concentration of CO_2 in the mixture (0,1,5,20%) at the same discharge power.

been confirmed as described earlier. For this process, the formation of long-lived NCO radical, ON–NCO or a similar intermediate, is important. Regarding the NCO radical, its rate coefficient is unknown and we had no possible means of measuring it. The reaction rate is dependent on the type of process which leads to NCO formation. One possible process is the thermal decomposition of $(HNCO)_3$[23] which can also be formed as a component of a complex reactions in the combustion process connected with the formation of NO_x prompt.[28] The long lifetime of the radical is also reported here. The main absorption bands of NCO are at 2300–2180 ν_{as} (s), 1505–1195 ν_s (w) and 715–580 cm^{-1} (s).[29] For the possible formation of trivial amino acids in the discharge, the presence of water is necessary, as the reaction of the NCO radical with water leads to the formation of an amide group, the essential component of amino acids. As the spectrometric analysis of the gas mixtures was performed only in the experiments where no explicit injection of water was used and only the residual humidity in the environment was present, the absorption bands related to amino acids had weak absorption, compared with our previous experiments in a more humid environment.[13,26] The identification of amino acids or their traces in the discharge volume was also complicated due to their possible polarization and the formation of zwitter ions, i.e., $NH_2^+COO^-$ or NH_3COO^-, in the presence of the electric field. This phenomenon results in the shifting of bands in the infrared spectra (*e.g.*, protonated amino cation NH_3^+ is shifted down to 2500 cm^{-1} and NH_2^+ to 2700 cm^{-1}), making possible analysis even more difficult. Furthermore, amino acids can be neutral, acidic or basic, depending on the number of NH_2^+ and COO^- groups in the structure of the molecule, and this can also have different effects on the infrared spectra.

Considering the entire region of the infrared absorption spectra, there were several bands, in addition to those aforementioned, which attracted our attention. First, in the left region of the spectra (Fig. 13), there were bands of amine NH_2, the zwitter ion NH_3^+ in the regions of 3490 and 3467, and 2580 and 2550 cm^{-1} respectively, while the region around 1900 cm^{-1} was dominated by NO, namely, an NO monomer band at 1920–1900 cm^{-1} and an NO dimer at 1840 cm^{-1}.

The region from 2000 cm^{-1} down to 1600 cm^{-1} (Fig. 14) is the region of carbonyls (ketones, esters, carboxylic acids, etc.), i.e., the compounds containing the C=O group. This region, particularly in the range of 1850 to 1600 cm^{-1}, is very important as it is the region of carbonyls with the double bond, which are very strongly dependent on their surroundings and their associations which govern their position and eventual shift of the absorption bands in the spectra. In our case, the bands visible in the spectra were carbonyl of carboxylic acid at 1720 cm^{-1}, carbonyl of imide at 1700 cm^{-1} (which is stronger as it occurs twice in one compound) and carbonyl of non-specified neutral amino acids at 1680 cm^{-1}. At the bottom edge of this region, a strong band of NO_2 occurred at 1630–1620 cm^{-1} along with C=C, C=N conjugated and carboxylate ion COO^- (ν_{as}). On the right-hand side of the NO_2 absorption band, a small band representing the amide I was observed (1640 cm^{-1}), which was quite visible, particularly in the spectra of the N_2–NO–CO_2 mixture. In the other two mixtures with initial O_2, a significant production of NO_2 caused the amide I band to interfere with the band of NO_2 and thus it remained invisible.

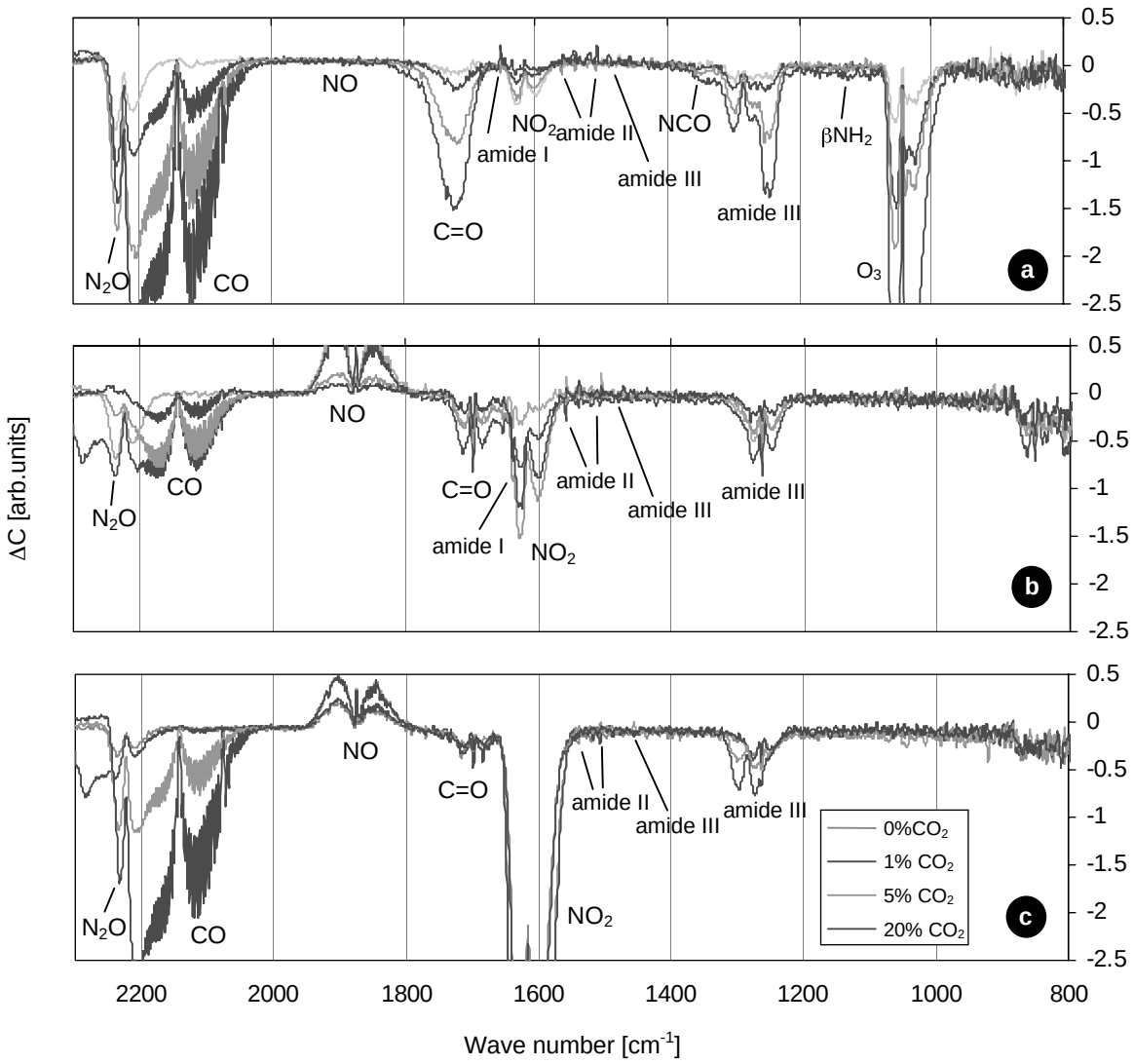

Fig. 14. Details of differential spectra of mixtures treated by DC positive corona discharge: (a) N_2–O_2–CO_2, (b) N_2–NO–CO_2, (c) N_2–NO–O_2–CO_2. Each curve represents a different concentration of CO_2 in the mixture (0,1,5,20%) at the same discharge power.

Going further down in the spectra into the region of 1600–1300 cm^{-1} (Fig. 14), at first the absorption band of amide II ($\beta\delta NH_x$) could be found in the region of 1600 to 1500 cm^{-1}. Here, the region 1560–1510 cm^{-1} in particular was full of random absorptions which corresponded to amide II. Further, in all types of mixtures, a small band at 1460 cm^{-1} was observed, which represented the combination of several bands with the central standard amide III band in its neutral state. The other components of this composition were the NCO radical, the imide group at 1490 cm^{-1} and the carboxylate ion COO^- (ν_s) at 1465 cm^{-1}. As amide III consists of two parts, one bound to a carbonyl group and another to NH_2, if the zwitter ion amino acid is formed, the amino group shifts down to the region of 1300 to 1250 cm^{-1}, where it interferes with the C–N and C–O bands and an intense band is formed (the shift of the carbonyl group is negligible compared with the shift of the amino group). Finally, in the lower part of the spectra, a small and sometimes hardly visible absorption in the region of 1140 to 1130 cm^{-1} was formed, representing βNH_2 amine and amide III (νC–N(C)), which usually appears in the region of 1190 to 1038 cm^{-1}.

Unfortunately, it is not possible to describe directly the relationship between the initial gas composition and the appearance of products like amides (monomers), imides (dimers), NCO and amino acids. As already mentioned, the problem is very complicated for several reasons. An analysis may be possible for chemical reactions of the first order (i.e., those dependent on the initial concentrations) under equilibrium conditions; however, the plasma chemistry in the discharge is much more complicated. The conditions for equilibrium in the discharge are barely fulfilled, many chain reactions take place, and many of the reactions sequences remain incomplete because of the limited residence time of the mixture in the discharge reactor. The oxidation reactions in the initial phase of the process have a low activation energy and in such cases the impact of a single electron is usually sufficient for the reaction to proceed. For such processes, it is easy to evaluate the energy consumption and the dependence of products on the initial gas composition. However, the process in the N_2–NO–CO_2–O_2–(H_2O) system consists mainly of chain reactions. The activation energy for molecular nitrogen is relatively high and several electrons are needed for its formation. Metastable molecules are

accumulated in the discharge (energy reservoir). This causes the time shift of the chemistry concerning electric parameters, which makes an evaluation based on the electrical parameters impractical. The chemical process is postponed, which results in the deformation of its dependence on energy delivery.

Regarding the reaction kinetics, we assume that for the formation of amino acids, approximately 10–15 reaction steps are needed, depending on the type of amino acid; for the formation of solid products, even more reaction steps are needed. This is also a very strong argument against the possible determination of the reaction constant. Therefore, at present, the only possible means of explaining the process is given in Fig. 6.[26)]

4. Conclusions

The positive DC corona discharge in the hemicylindrical type reactor geometry was used.

The experimental results and the analysis performed confirmed that CO_2 influenced the discharge character as well as the chemical processes inside the reactor, and therefore also influenced the final products.

Analysis and identification of the products were performed along with the evaluation of the concentration changes of the main components of the gas mixture. Among the products of the process, the amides I–III, amines, imide, NCO and ozone were found, which confirmed the assumption of the possible formation of the amino acids or their fractions in the discharge process.

The present paper has shown that measurements in the simple N_2–NO system are not sufficiently relevant to evaluate the deNO_x process for practical use, because the addition of a particular component into the gas mixture can change the mechanism of the discharge and its influence on the gas mixture completely.

In the case of the N_2–NO gas mixture, the chemical process is fully oxidative, while after CO_2 is introduced, the reaction character changes to oxidation-reduction with the focus on oxidation. This fact is very important, since in the combustion process, along with the nitrogen oxides, the CO_2 and the water are also present. The water stabilizes the formation of the amino acids and supports the formation of the solid product insoluble in the water.

The fact that this process is also possible in the presence of oxygen in the system is very important particularly for diesel engines and lean mixture combustion processes.

The process described in the present paper as leading to the formation of amino acids is possible and is closely related to the process in the primary atmosphere, very similar to that involving flue gases, which led to the origin of life on Earth.[30)]

Acknowledgement

The project was partially supported by a Grant-in-Aid from the Ministry of Education, Culture, Sports, Science and Technology (Japan), and Grant Project 1/8312/01 of MSV SR (Slovakia).

1) R. H. Amirov: Proc. 21st ICPIG, Bochum, 1993, Vol. 2, p. 114.
2) L. Civitano: *Non-Thermal Plasma Techniques for Pollution Control*, eds. B. Penetrante and S. E. Schultheis (Springer, New York, 1993) NATO Series, Vol. 1, p. 103.
3) S. Masuda and H. Nakao: IEEE Trans. Ind. Appl. **26** (1990) 374.
4) J. S. Chang: IEEE Trans. Plasma Sci. **19** (1991) 1152.
5) A. Jaworek, J. Mizeraczyk, A. Krupa and T. Czech: Czech J. Phys. **45** (1995) 1049.
6) K. Kato, Y. Kasuga, M. Fujiwara and K. Onda: Trans. IEE Jpn. A **116** (1996) 94.
7) A. Mizuno, K. Shimizu and A. Chakrabarti: IEEE Trans. Ind. Appl. **31** (1995) 957–963.
8) B. M. Penetrante, M. C. Hsiao and B. T. Merritt: IEEE Trans. Plasma Sci. **23** (1995) 679.
9) M. Rea and K. Yan: *Non-Thermal Plasma Techniques for Pollution Control*, eds. B. Penetrante and S. E. Schultheis (Springer, New York, 1993) NATO Series, Vol. 1, p. 191.
10) W. R. Rutgers: Proc. 21st ICPIG, Bochum, 1993, Vol. 3, p. 70.
11) E. M. Veldhuizen, W. R. Rutgers and V. A. Bityurin: Plasma Chem. & Plasma Process. **16** (1996) 227.
12) G. E. Vogtlin and B. M. Penetrante: *Non-Thermal Plasma Techniques for Pollution Control*, eds. B. Penetrante and S. E. Schultheis (Springer, New York, 1993) NATO Series, Vol. 2, p. 187.
13) M. Morvová: J. Phys. D **31** (1998) 1865.
14) A. Huczko, A. Resztak and T. Opalinska: Proc. Hakone II, Kazimierz, 1987, p. 110.
15) M. Arquilla: Proc. ISPC-11, Loughborough, 1993, p. 593.
16) M. Morvová: Proc. 10th SEPCRLTP, Stará Lesná, 1994, p. 155.
17) M. Morvová: Proc. Hakone VII, Greifswald, 2000, Vol. 2, p. 513.
18) A. Lofthus and P. H. Krupenie: J. Phys. Chem. Ref. Data **6** (1977) 113.
19) F. Hanic, M. Morvová and M. Morva: J. Therm. Anal. Calor. **60** (2000) 1111.
20) Z. Machala: PhD Thesis, Paris-Sud University, Orsay, 2000.
21) P. Veis: PhD Thesis, Paris-Sud University, Orsay, 1993 [in French].
22) S. De Benedictis, G. Dilecce and M. Šimek: J. Phys. D **30** (1997) 2887.
23) R. A. Perry: J. Chem. Phys. **82** (1985) 5485.
24) R. A. Perry and D. L. Siebers: Nature **324** (1986) 657.
25) T. Oda, T. Takahashi and R. Yamashita: J. Adv. Oxid. Technol. **2** (1997) 227.
26) M. Morvová, F. Hanic and I. Morva: J. Therm. Anal. Calor. **61** (2000) 273.
27) J. J. Lowke and R. Morrow: Aust. J. Phys. **48** (1995) 403.
28) W. F. Cooper and J. F. Hershberger: J. Phys. Chem. **96** (1992) 771.
29) G. Socrates: *Infrared Characteristic Group Frequencies* (John Wiley & Sons, Chichester, 1994) 2nd ed., p. 240.
30) S. L. Miller: J. Am. Chem. Soc. **77** (1955) 2351.